Metal-ion induced alignment of an orthogonal anthracene–pyrimidine derivative. Cooperation of metal coordination, hydrogen bonding, and aromatic stacking in the buildup of one-, two- and three-dimensional networks

Takayoshi Ezuhara, Ken Endo, Osamu Hayashida and Yasuhiro Aoyama*

CREST, Japan Science and Technology Corporation (JST), Institute for Fundamental Research of Organic Chemistry, Kyushu University, Hakozaki, Higashi-ku, Fukuoka 812-81, Japan

9-(5-Pyrimidinyl)anthracene (**1**) forms a ternary adduct **1** · $Cd(NO_3)_2 \cdot 2(CH_3OH)$, the crystal structure of which shows a remarkable cooperation of metal coordination, hydrogen bonding and aromatic stacking interactions in the hierarchical formation of one-, two- and three-dimensional networks. Ditopic pyrimidine ligands and cadmium ions form a pyrimidine–Cd^{2+} alternate copolymeric chain. The chains are held together to give a sheet by extensive cross-links *via* hydrogen bonding between metal-bound nitrate ions of one chain and methanol molecules of the neighboring one. The sheets are self-assembled *via* stacking, interpenetration or intercalation of the orthogonal anthracene side arms on both sides of a sheet. This gives rise to a layered structure having an alternate arrangement of inorganic and organic sheets; the former contains Cd^{2+} ions two-dimensionally networked by pyrimidine bridges and hydrogen-bonded nitrate–methanol links, while the latter is composed of tightly-packed anthracene columns.

Hydrogen bonding is extensively used to control crystal structures.[1] Since it is monovalent, highly substituted or multifunctional molecules are required in order to achieve higher dimensional, three- > two- > one-dimensional (3D > 2D > 1D), networks.[1] Metal coordination is another potential network-forming strategy.[2] It is multivalent. In addition, metal-bound ligands are often also involved in hydrogen bonding,[1a,3] thus enhancing network dimensionalities.

We have been concerned with functional crystal structure control, particularly aiming at designing aromatic stacks and columns using orthogonal anthracene–resorcinol derivatives.[4] In the present work, we have prepared an analogous anthracene–pyrimidine derivative **1** and studied how aromatic (anthracene) stacking cooperates with metal-ion coordination at the pyrimidinyl sites. We report here that a hierarchical buildup of 1D, 2D and 3D networks results in an inorganic–organic layer structure.

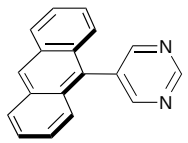

1

Results and Discussion

Crystal structure of 1 · $Cd(NO_3)_2 \cdot 2(CH_3OH)$

Compound **1** was prepared by the reaction of 9-bromoanthracene with 5-trimethylstannylpyrimidine, which in turn was obtained by the stannylation of 5-bromopyrimidine with hexamethyldistannane. Treatment of compound **1** with cadmium nitrate in methanol–water affords a 1 : 1 adduct containing two molecules of the solvent, *i.e.*, **1** · $Cd(NO_3)_2 \cdot 2(CH_3OH)$ as yellow needles. It crystallizes in the space group $P2_1/n$ (monoclinic).[5] The cadmium ion is hexacoordinate with two pyrimidine ligands in the apical positions and two nitrate ions (*cis*) and two methanol molecules (*cis*) in the equatorial positions, thus forming an N_2O_4 octahedral coordination sphere (Fig. 1). Table 1 shows the atomic coordinates and important bond lengths and angles. Particularly, the anthracene and the pyrimidine rings are not perpendicular, the dihedral angle being 56°. The crystal structure is summarized as follows.

Pyrimidine–Cd^{2+} alternate copolymeric 1D chains

Both nitrogen atoms in a pyrimidine ring coordinate to a Cd^{2+} ion, which in turn links two pyrimidine ligands *via* an N—Cd^{2+}—N bridge. This leads to a pyrimidine–Cd^{2+} alternate copolymeric 1D chain [Fig. 2; front view (*a*) and side

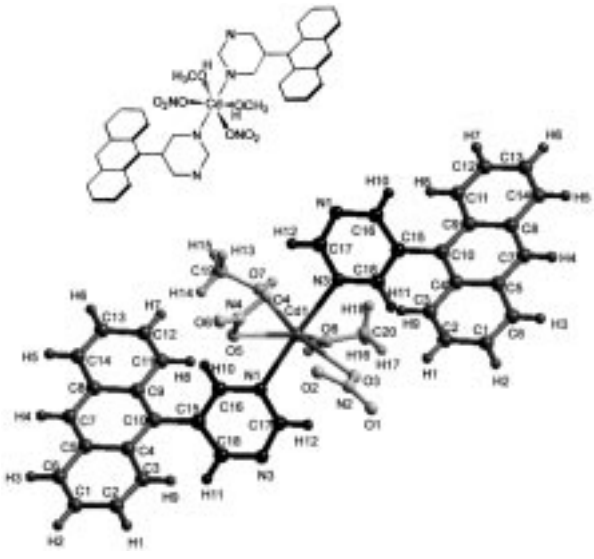

Fig. 1 Coordination geometry around a cadmium ion

* Fax: +81-92-642-2719; E-mail: aoyamay@ms.ifoc.kyushu-u.ac.jp

Table 1 Atomic coordinates and important bond lengths (Å) and angles (°) in $\mathbf{1} \cdot Cd(NO_3)_2 \cdot 2(CH_3OH)$.[a]

Atom	x/a	y/b	z/c	Atom	x/a	y/b	z/c
Cd(1)	0.48886(7)	0.25207(2)	0.26349(5)	C(5)	0.286(1)	0.5155(3)	−0.1045(8)
O(1)	0.574(1)	0.1396(3)	−0.0001(9)	C(6)	0.325(1)	0.5409(3)	−0.2226(9)
O(2)	0.663(1)	0.2078(3)	0.0956(8)	C(7)	0.254(1)	0.5419(3)	0.0039(8)
O(3)	0.4273(9)	0.1758(2)	0.1433(6)	C(8)	0.2161(10)	0.5184(3)	0.1148(8)
O(4)	0.847(2)	0.2743(4)	0.3062(10)	C(9)	0.202(1)	0.4636(3)	0.1159(7)
O(5)	0.693(1)	0.3191(4)	0.204(1)	C(10)	0.2388(9)	0.4357(3)	0.0080(7)
O(6)	0.959(1)	0.3217(4)	0.186(1)	C(11)	0.152(1)	0.4412(3)	0.2336(8)
O(7)	0.4376(10)	0.3098(2)	0.4261(6)	C(12)	0.121(1)	0.4691(4)	0.3354(8)
O(8)	0.2066(9)	0.2309(3)	0.3130(8)	C(13)	0.138(1)	0.5224(4)	0.3351(9)
N(1)	0.3261(8)	0.3004(2)	0.1075(6)	C(14)	0.182(1)	0.5458(3)	0.2301(9)
N(2)	0.554(1)	0.1733(3)	0.0781(7)	C(15)	0.2336(10)	0.3794(3)	0.0092(7)
N(3)	0.6203(8)	0.1997(2)	0.4252(6)	C(16)	0.3339(10)	0.3515(3)	0.1016(7)
N(4)	0.837(1)	0.3062(3)	0.2257(9)	C(17)	0.220(1)	0.2772(3)	0.0197(7)
C(1)	0.361(1)	0.5144(4)	−0.3270(8)	C(18)	0.625(1)	0.1489(3)	0.4229(7)
C(2)	0.362(1)	0.4614(3)	−0.3231(8)	C(19)	0.521(2)	0.3568(5)	0.464(1)
C(3)	0.324(1)	0.4354(3)	−0.2190(8)	C(20)	0.142(2)	0.1881(5)	0.360(2)
C(4)	0.2810(10)	0.4612(3)	−0.1050(7)				
Cd(1)—O(3)	2.389(7)	Cd(1)—O(8)	2.359(7)	Cd(1)—N(3)	2.330(6)	O(4)—O(8)[b]	3.00(3)
Cd(1)—O(5)	2.49(1)	Cd(1)—N(1)	2.330(6)	O(1)—O(7)[b]	3.27(2)	O(6)—O(8)[b]	3.26(2)
Cd(1)—O(7)	2.341(6)			O(2)—O(7)[b]	2.93(2)		
O(3)—Cd(1)—O(5)	124.3(3)	O(5)—Cd(1)—O(7)	83.0(3)	O(7)—Cd(1)—O(8)	76.6(3)	O(8)—Cd(1)—N(1)	80.5(2)
O(3)—Cd(1)—O(8)	77.1(2)	O(5)—Cd(1)—N(1)	75.5(3)	O(7)—Cd(1)—N(1)	91.8(2)	O(8)—Cd(1)—N(3)	92.7(3)
O(3)—Cd(1)—N(1)	91.6(2)	O(5)—Cd(1)—N(3)	111.1(3)	O(7)—Cd(1)—N(3)	87.4(2)	N(1)—Cd(1)—N(3)	173.2(2)
O(3)—Cd(1)—N(3)	86.0(2)						

[a] Atomic coordinates of hydrogen atoms were excepted. [b] Hydrogen bond distance

view (*b*) with their schematic explanations (*a*′) and (*b*′) and top view (*c*) of view (*b*), where and hereafter anthracene rings, pyrimidine rings, nitrate ions, methanol molecules and cadmium ions are shown in red, blue, yellow, green and pink, respectively]. The anthracene rings are all parallel, being kept at an angle of 53.5° with respect to the column axis. They are alternately located in the left (front) and right (rear) sides of the chain with a separation of $I_a^1 = 12.33$ Å.

Interchain nitrate–methanol hydrogen bonding to give 2D sheets

All the metal-bound nitrate ions and methanol molecules are located on the same sides of the chain [Fig. 2(*b*) and 2(*c*)], and they form interchain hydrogen bonds (Fig. 3). The pyrimidine–Cd^{2+} chains are thus held together to give a sheet [Fig. 4; front view (*a*) and top view (*b*)]; interchain distances are $I_n(p) = 6.50$ and $I_n(nm) = 5.18$ Å for the pyrimidine chains and nitrate–methanol chains, respectively. Another notable consequence of the sheet formation is that the anthracene rings sticking out vertically on both sides of the sheet form loosely-packed columns in the direction of arrows with center-to-center and face-to-face inter-ring distances of $^cI_a^2 = 7.73$ and $^fI_a^2 = 7.23$ Å and a tilt angle of 69.3° with respect to the column axis.

Intersheet aromatic stacking to give 3D layers

Two surfaces of neighboring sheets then self-assemble *via* stacking; the interpenetration or intercalation of the orthogonal anthracene moieties is shown (top views) in Fig. 5 [schematic representation (*a*) and actual structures (*b*) and (*c*)], where anthracene rings on two neighboring sheets are shown in red and purple for clarity. The loosely-packed aromatic columns on one sheet become tighter. This occurs on both sides of a sheet and hence leads to a layer structure of the crystal, composed of alternating inorganic and organic sheets with an intersheet distance of $I_s = 6.59$ Å [Fig. 5(*b*)]. The inorganic sheet contains Cd^{2+} ions 2D-networked *via* pyrimidine bridges and hydrogen-bonded nitrate–methanol links, a space filling model of which is shown in Fig. 6(*a*). The organic sheet is composed of parallel-aligned anthracene columns with $^cI_a^3 = 3.86$ and $^fI_a^3 = 3.62$ Å and an intercolumn distance of $I_c = 10.37$ Å [Fig. 6(*b*)].

Orthogonality strategy

Molecular networking[1–4] is becoming an important general strategy of crystal engineering. The structure of a network depends, and is hence predictable at least to some extent, on the topology of intermolecular interaction of constituent molecules. Construction of diamondoid lattices from tetrahedrally substituted molecules provides one of the best examples.[6] The essence of the orthogonality strategy[3] lies in the orthogonal arrangement, using biaryl general structures, of a functional aromatic moiety (anthracene) and a network-forming interaction site (pyrimidine). Such a structural aspect of the molecule results in a kind of 'phase separation' in the crystal structure. The pyrimidine sites maintain inorganic supporting sheets, while the anthracene moieties orthogonal to the sheets form tightly packed organic layers. From a different viewpoint, an inorganic sheet is maintained in a sandwich manner by the highly-orienting aromatic layers. This is due to a remarkable cooperation of metal coordination, hydrogen bonding and aromatic stacking interactions in a hierarchical buildup of 1D, 2D and 3D networks.

Experimental

9-(5-Pyrimidinyl)anthracene 1

This compound was prepared in a similar manner to its *bis*-pyrimidine analogue, *i.e.*, 9,10-bis(5-pyrimidinyl)anthracene.[1a] Into a solution of 9-dibromoanthracene (1.7 g, 6.6 mmol) and dichlorobis(triphenylphosphine)palladium(II) (0.15 g, 0.21 mmol) in dry benzene (25 mL) and dry THF (25 mL) was added a THF solution (50 mL) of 5-trimethylstannylpyrimidine (1.7 g, 7.0 mmol) in a period of 25 min at

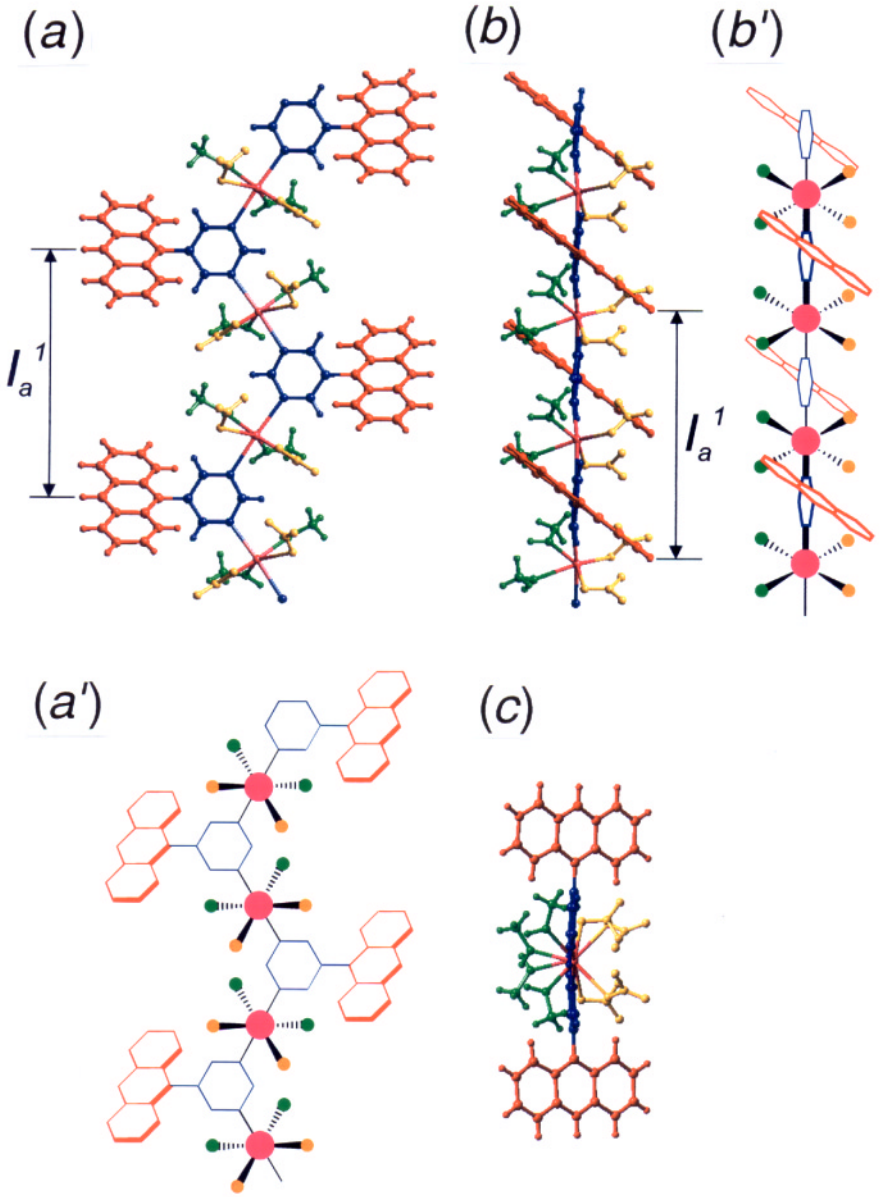

Fig. 2 Formation of a pyrimidine–Cd^{2+} alternate copolymeric chain: front view (*a*) and side view (*b*) with its top view (*c*) and schematic explanations of views (*a*) and (*b*) [(*a*′) and (*b*′)]

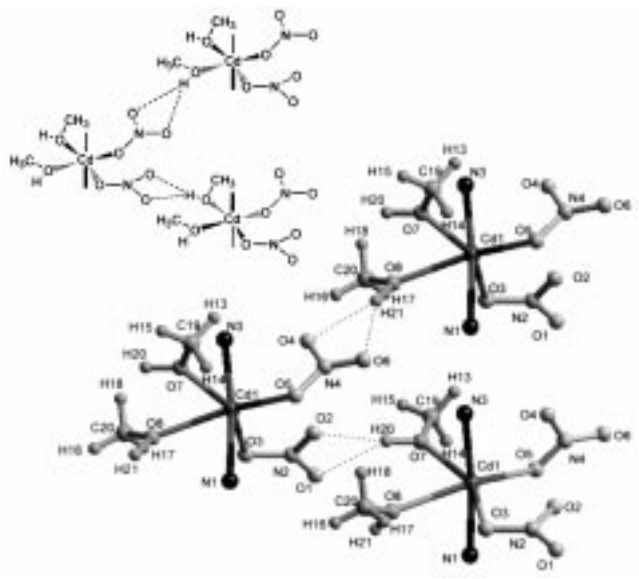

Fig. 3 Hydrogen bonds between Cd^{2+}-coordinated nitrate ions and methanol molecules

room temperature under nitrogen.[7] The mixture was stirred at 75 °C for 10 d and then cooled down to room temperature. Diethyl ether was added and the mixture was washed with a saturated aqueous sodium chloride solution, dried on sodium sulfate, and evaporated to dryness. Purification of the residue by means of chromatography on silica gel with a mixed solvent of hexane and ethyl acetate (1 : 1) as eluant, followed by recrystallization from dichloromethane–hexane (1 : 4), gave compound **1** (0.70 g, 41%) as pale yellow plates. M.p. 149–151.5 °C: IR (KBr): 1550 cm^{-1}; ^1H NMR [$(CD_3)_2SO$]: δ 7.49 (d, 4 H), 7.57 (m, 2 H), 8.20 (d, 2 H), 8.80 (s, 1 H), 8.93 (s, 2 H), 9.43 (s, 2 H). Anal. calc (%) for $C_{18}H_{12}N_2$: C 84.35; H 4.72; N 10.93. Found: C 83.68; H 4.72; N 10.72.

Compound **1** (64 mg, 0.25 mmol) was added to a solution of $Cd(NO_3)_2 \cdot 4H_2O$ (770 mg, 2.5 mmol) in methanol (2 mL) and water (2 mL). The mixture was refluxed under nitrogen. A minimal amount of butan-1-ol was added to make a clear solution. The mixture was allowed to cool down to room temperature to give single crystals of the adduct **1** · $Cd(NO_3)_2 \cdot 2(CH_3OH)$ (40 mg, 29%) as yellow needles. IR (KBr): 1380, 1580 cm^{-1}: ^1H NMR [$(CD_3)_2SO$] δ 3.16 (s, 6 H, methanol) in addition to those for compound **1**. Anal. calc (%) for $C_{20}H_{20}N_4O_8Cd$: C 43.14; H 3.62; N 10.06. Found C 42.83; H 3.53; N 10.05.

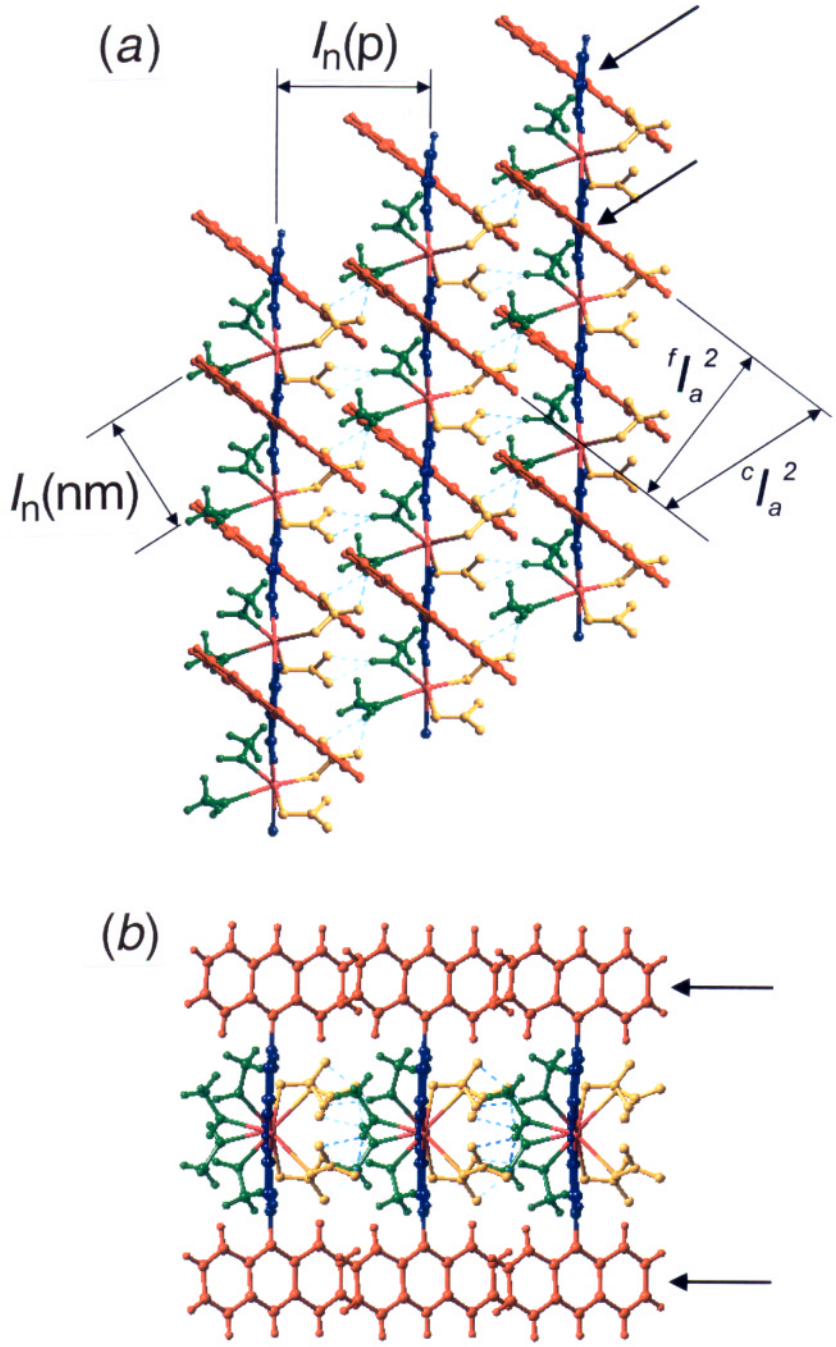

Fig. 4 Alignment of pyrimidine–Cd^{2+} chains to give a sheet *via* interchain hydrogen bonding between metal-bound nitrate ions and methanol molecules: front view of a sheet (*a*) and its top view (*b*)

X-Ray crystallography

Diffraction data were collected with a Rigaku AFC7R four-circle automated diffractometer with graphite-monochromated Mo-Kα (λ = 0.71069 Å) radiation. Single crystals suitable for X-ray analysis were mounted on a glass fiber by use of an epoxy adhesive. A linear absorption correction was applied in each case. The intensities of three standard reflections were monitored after every 150 reflections; the decays of intensities were within 2%. The intensity data collected by using the ω scan technique were corrected for both Lorentz and polarization effects. An absorption correction was also applied with the program PSI.

The structure was solved using of the direct-methods program SAPI90 and expanded DIRDIF94. Non-hydrogen atoms were refined anisotropically by full-matrix least-squares calculations. Hydrogen atoms were located from difference-Fourier maps and their parameters were refined isotropically. The weighting scheme of $w^{-1} = \sigma^2(F_o) + 0.00144|F_o|^2$ was employed. Atomic scattering factors and anomalous dispersion terms were taken from International Tables for X-ray Crystallography. All calculations were performed on an INDY workstation by using the teXsan crystallographic software package of the Molecular Structure Corporation. Crystal structures were visualized on an INDY workstation using the Cerius2 set of computer programs of Molecular Simulations Incorporated.

CCDC reference number 440/003.

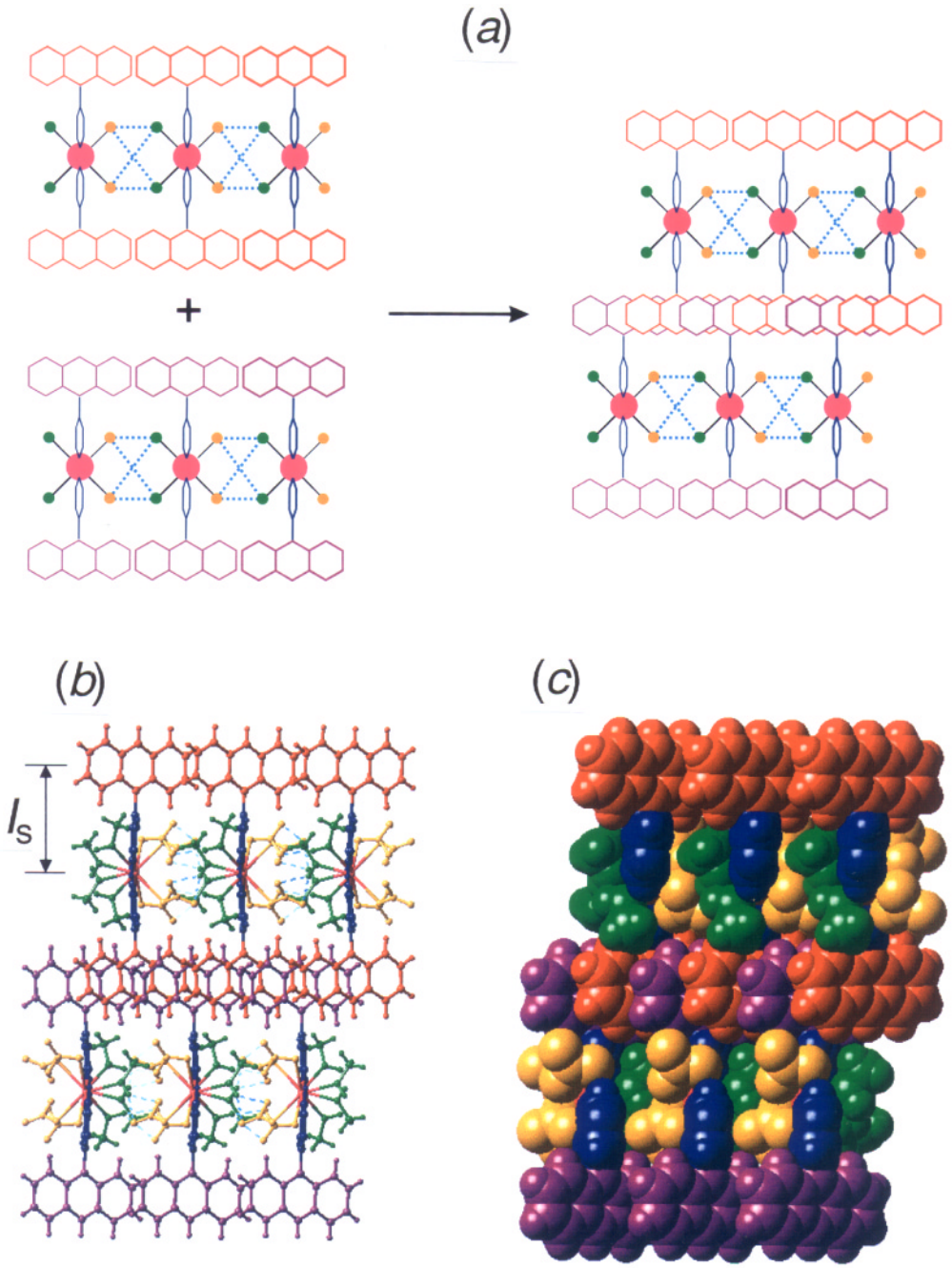

Fig. 5 Top views of self-assembly of sheets *via* stacking, interpenetration or intercalation of anthracene moieties vertically sticking out: schematic representation (*a*) and actual structures (*b*) and (*c*)

Acknowledgements

This work was supported by CREST (Core Research for Evolutional Science and Technology) of Japan Science and Technology Corporation and also by a Grant-in-Aid for COE Research 'Design and Control of Advanced Molecular Assembly Systems' from the Ministry of Education, Science and Culture, Japan (#08CE2005).

References

1 (*a*) For a list of recent literature on the formation of ordered crystal structure involving hydrogen-bonded 1D, 2D, and 3D motifs, see: Y. Aoyama, K. Endo, T. Anzai, Y. Yamaguchi, T. Sawaki, K. Kobayashi, N. Kanehisa, H. Hashimoto, Y. Kai and H. Masuda, *J. Am. Chem. Soc.*, 1996, **118**, 5562; (*b*) J. C. MacDonald and G. M. Whitesides, *Chem. Rev.*, 1994, **94**, 2383.

2 *Comprehensive Supramolecular Chemistry*, ed. J. M. Lehn, Pergamon Press, Oxford, 1996, vol. 9. ch. 2, 4, 5, 6 and 7. See also: R. Robson, B. F. Abrahams, S. R. Batten, R. W. Gable, B. F. Hoskins and J. Liu. in *Supramolecular Architecture*, ed. T. Bein, ACS Symposium Series 499, American Chemical Society, Washington DC, 1992, ch. 19; M. Fujita and K. Ogura, *Bull. Chem. Soc. Jpn.*, 1996, **69**, 1471; M. Fujita and K. Ogura, *Coord. Chem. Rev.*, 1996, **148**, 249.

3 Y. Aoyama, K. Endo, K. Kobayashi and H. Masuda, *Supramol. Chem.*, 1995, **4**, 229; K. Endo, T. Sawaki, M. Koyanagi, K. Kobayashi, H. Masuda and Y. Aoyama, *J. Am. Chem. Soc.*, 1995, **117**, 8341; K. Endo, T. Ezuhara, M. Koyanagi and Y. Aoyama, *J. Am. Chem. Soc.*, 1997, **119**, 449.

4 L. P. Wu, M. Yamamoto, T. Kuroda-Sowa, M. Maekawa, J. Fukui and M. Munakata, *Inorg. Chim. Acta*, 1995, **239**, 165; M. Mitsumi, J. Toyoda and K. Nakasuji, *Inorg. Chem.*, 1995, **34**, 3367; M. Munakata, L. P. Wu, M. Yamamoto, T. Kuroda-Sowa and M. Maekawa, *J. Am. Chem. Soc.*, 1996, **118**, 3117.

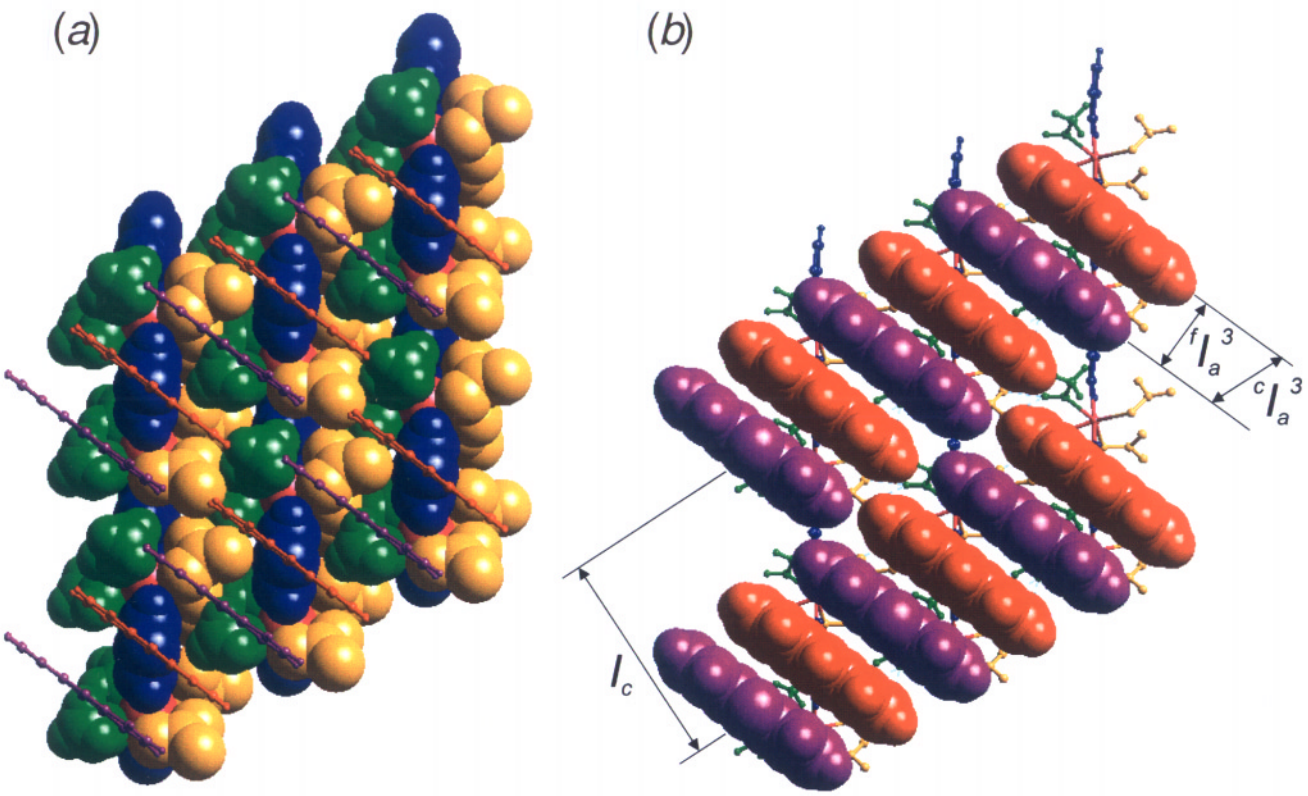

Fig. 6 Front views of an inorganic sheet (*a*) and an organic sheet (*b*)

5 Crystal parameters: $a = 7.729(1)$, $b = 26.347(1)$, $c = 19.420(1)$ Å, $\beta = 95.78(1)°$, $U = 2111.0(4)$ Å^3, $Z = 4$, $d_{calc} = 1.75$, no. unique reflections = 4962, no. reflections used = 2411, $R = 0.044$, $R_w = 0.066$, Goodness of fit = 1.22.

6 O. Ermer, *J. Am. Chem. Soc.*, 1988, **110**, 3747; M. Simard, D. Su and J. D. Wuest, *J. Am. Chem. Soc.*, 1991, **113**, 4696; M. Zaworotko, *J. Chem. Soc. Rev.*, 1994, **23**, 283.

7 H. Azizian, C. Eaborn and A. Pidcock, *J. Organomet. Chem.*, 1981, **215**, 49.

Received 2nd *June* 1997; *Paper* 7/07634G